Applied Geochemistry 124 (2021) 104812

Contents lists available at ScienceDirect

Applied Geochemistry

journal homepage: http://www.elsevier.com/locate/apgeochem

Natural analogue evidence for controls on radionuclide uptake by fractured crystalline rock

Richard Metcalfe [a,*], Antoni E. Milodowski [b], Lorraine P. Field [b], Roy A. Wogelius [c], Gráinne Carpenter [d], Bruce W.D. Yardley [e], Simon Norris [f]

[a] Quintessa Limited, Videcom House, Newtown Road, Henley-on-Thames, Oxfordshire, RG9 1HG, UK
[b] British Geological Survey, Environmental Science Centre, Nicker Hill, Keyworth, Nottingham, NG12 5GG, UK
[c] School of Earth, Atmospheric, and Environmental Sciences, University of Manchester, Manchester, M13 9PL, UK
[d] NSG Environmental Ltd, Festival House, Jessop Avenue, Cheltenham, Gloucestershire, GL50 3SH, UK
[e] School of Earth and Environment, University of Leeds, Leeds, LS2 9JT, UK
[f] Radioactive Waste Management Limited, Building 587, Curie Avenue, Harwell Science and Innovation Campus, Didcot, Oxfordshire, OX11 0RH, UK

ARTICLE INFO

Editorial handling by Prof. M. Kersten

Keywords:
Rock matrix diffusion
Retardation
Radionuclide
Groundwater
Crystalline rock

ABSTRACT

Fractured Crystalline Rocks (FCR) are being considered in several countries as hosts for radioactive waste repositories. In FCR, radionuclides may be transported relatively rapidly by bulk groundwater flow through open fractures, but much more slowly by diffusion through porewater in the rock matrices. Rock matrix diffusion (RMD) is the diffusion of radionuclides in the aqueous phase, between open fractures and rock matrices. Sorption or co-precipitation on the fracture surfaces and walls of the matrix pores causes further radionuclide retardation. RMD may be important in a repository's safety case and has been investigated by many published short-term (to a few years) laboratory and *in-situ* experiments. To improve understanding over longer timescales, we investigated evidence for RMD of several natural radioelements, and radioelement analogues, in five exemplar fractured crystalline rock (FCR) samples aged between c. 70 Ma and c. 455 Ma. The sample suite consisted of two samples of Borrowdale Volcanic Group (BVG) meta-tuff from northwest England, a sample of Carnmenellis Granite from southwest England and two samples of Toki Granite from central Japan. Uptake or loss of the studied elements is limited to an altered damage zone in each sample, coupled to mineral alteration processes. These zones are most extensive (a few tens of millimetres) in the Toki Granite samples. We also found unstable primary igneous minerals to persist in the immediate wallrocks of fractures in studied granite samples, suggesting that pores were not permanently water saturated in these samples. Although only a small sample suite was studied, the results show that while RMD may be important in some kinds of FCR, in others it may be negligible. Site-specific information is therefore needed to determine how much reliance can be placed on RMD when developing a safety case.

1. Introduction

For a deep (typically 500 m or more) radioactive waste repository constructed in Fractured Crystalline Rock (FCR) the rock's ability to retard or incorporate radionuclides migrating out of the engineered barrier system could be an important component of the safety case (SKB, 2010; Posiva, 2013; RWM, 2016). Generally, understanding solute retardation and incorporation within FCR is necessary to model contaminants released into them from waste (Bear et al., 1993; Mutch et al., 1993).

In FCR, groundwater can flow only through transmissive fractures (Sharp, 2014), generally a small proportion of the rock (e.g. <0.5% of the rock volume in the Borrowdale Volcanic Group (BVG) of northwest England; Milodowski et al., 1997). Radionuclides dissolved in the groundwater may be retarded by sorbing onto mineral surfaces that line fractures, or by incorporation into minerals that precipitate in the fractures. However, retardation can be enhanced if the radionuclides diffuse from the fractures into the rock matrix, a process termed rock matrix diffusion (RMD). Radionuclides may be retarded in the matrix because the pore water into which the they diffuse is stagnant, because they sorb onto mineral surfaces, or because they are incorporated into secondary minerals formed by interactions between the rocks,

* Corresponding author.
E-mail address: richardmetcalfe@quintessa.org (R. Metcalfe).

https://doi.org/10.1016/j.apgeochem.2020.104812
Received 27 July 2020; Received in revised form 26 October 2020; Accepted 29 October 2020
Available online 2 November 2020

waste-derived leachate and/or groundwater.

A safety assessment for a FCR-hosted radioactive waste repository requires transport and retardation processes to be understood. To investigate these processes, there have been many experimental programmes in surface and underground laboratories by radioactive waste management organisations, research institutes and universities (IAEA, 2001; NEA, 2013; Ikonen et al., 2017; Poteri et al., 2018). These experiments provide much of the necessary understanding but investigate timescales orders of magnitude shorter than that of a typical safety assessment (which typically considers 10^5–10^6 years quantitatively) and so may not capture the long-term behavior. Therefore, to complement the large body of experimental results, we have studied the behavior of solutes and radionuclides over much longer timescales, by carrying out "natural analogue" studies (Miller et al., 2000).

2. Existing conceptual models of rock matrix diffusion

Several concepts for radionuclide migration and retardation in fractured crystalline rock have been developed in various countries (Baker et al., 2002; Vilks et al., 2003; Winberg et al., 2003; SKB, 2010; Alexander et al., 2009; Poteri, 2009; Poteri et al., 2014; Tachi et al., 2015; RWM, 2016; Neretnieks, 2017). These differ in detail but generally treat diffusion as obeying Fick's laws and represent sorption using linear isotherms. Earlier models (Baker et al., 2002, Fig. 1) represented groundwater as advecting through planar fractures, with diffusion perpendicular to the fractures, directly into fresh wallrock.

Many assume uniform wallrock retention (sorption coefficients) and transport parameters (porosities, diffusion coefficients) with connected, water-saturated porosity throughout the wallrock, so that diffusion is not spatially limited. Sorption is assumed to occur onto minerals in the rock matrix. More recent conceptual models (Winberg et al., 2003; Poteri, 2009; Voutilainen et al., 2019) represent advection as focused in channels within fracture planes and identify layers with different retention (sorption coefficients) and transport parameters (porosities, diffusion coefficients) to reflect fracture lining minerals and/or altered wallrocks proximal to the fracture. These models also consider diffusion into stagnant water within poorly connected pores within fracture fills and/or wallrock.

Research in Finland, notably during the Palmottu natural analogue study, found that mineral-water reactions in fracture wallrocks in granite may affect the ability of the rock matrix to uptake radionuclides from flowing water (Kemppainen et al., 2001; Marcos et al., 2000; Ahonen et al., 2004; Markovaara-Koivisto et al., 2008; Read et al., 2008). Zones of rock matrix where these reactions have increased porosity were found to coincide with zones of U-uptake (Kemppainen et al., 2001; Markovaara-Koivisto et al., 2008). Furthermore, the results show that, depending on the groundwater conditions, significant porosity changes may occur over timescales that are short compared to those of safety assessment. For example, Marcos et al. (2000) report that within the last 10,000 years, U has accumulated in the weathered zone of granite boulders, where porosity is >1% compared to 0.4%–0.6% in the unweathered matrix. In particular, increased porosity was found in feldspars and biotite (Kemppainen et al., 2001; Markovaara-Koivisto et al., 2008). Changing groundwater conditions have also caused the re-mobilisation of U. Read et al. (2008) report evidence for U re-mobilisation in fractured granitic rocks during three time intervals (70–100 ka, 28–36 ka and <2500 years) at sites in southwest Finland, reflecting periods of influx of oxidizing water.

Published work shows that each of the models for radionuclide retention by RMD, sorption and mineral reactions can be valid for specific combinations of water/rock conditions and/or modelling purposes. Here we test whether observations on natural samples match these prior concepts and assess evidence for temporal changes in the importance of these processes.

3. Samples and methods

3.1. Approach

We investigated evidence for past transport and retardation of natural radioelements and analogues for radioelements in five exemplar samples of different types of FCR. Results were compared with expectations derived from published conceptual models of radionuclide/solute transport and retardation (Baker et al., 2002; Vilks et al., 2003; Winberg et al., 2003; Alexander et al., 2009; Poteri, 2009; Tachi et al., 2015; Voutilainen et al., 2019). The specimens were selected to represent a range of rock types in which groundwater moves in fractures. The contrasting rock characteristics are appropriate for testing whether existing

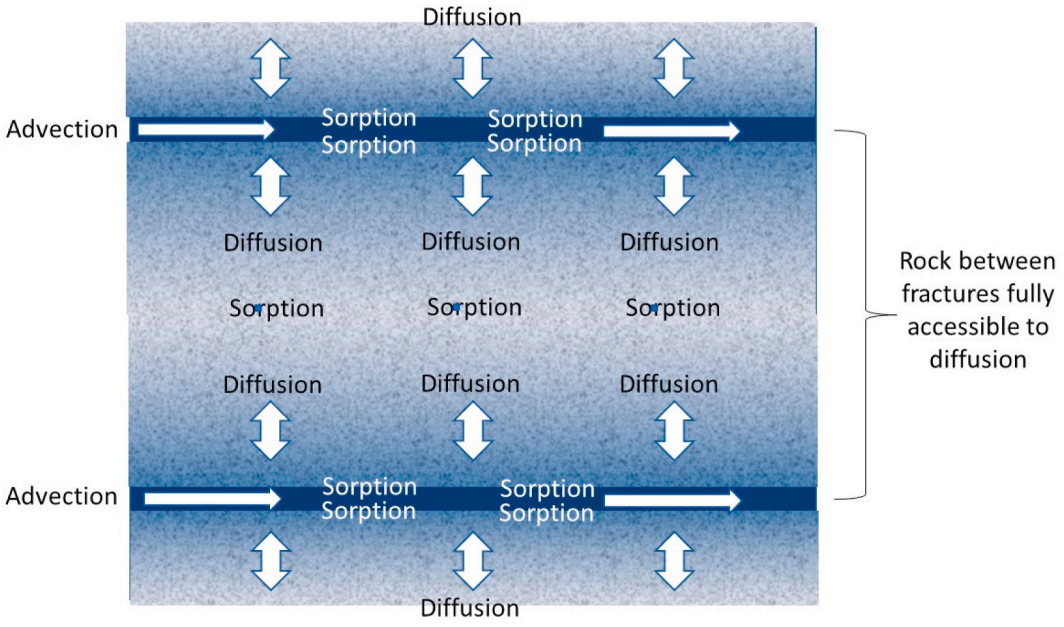

Fig. 1. Illustration of an example conceptual model for radionuclide uptake fractured crystalline rock (based on model described in Baker et al., 2002). Radionuclides can diffuse into or out from the rock matrix, depending upon the concentration gradient in the matrix porewater with respect to distance from the fracture.

Table 1
Summary of the studied samples.

Name	Locality	Sample No.	Age of host rock (Ma)	Sample Depth (m below ground level)	Rock Type	Fracturing and Alteration	Relative degrees of chemical reactivity of primary minerals, fracture complexity, extent of fracture wallrock alteration, groundwater fluxes (1 = least, 2 = intermediate, 3 = most)
Carnmenellis Granite	Rosemanowes Quarry, Cornwall, southwest England	SSK70951	310	2280	Fine to medium-grained granite	Planar fracture thinly coated by late-stage laumontite and calcite, consistent with low-temperature mineralization (Jove and Hacker, 1997) in the present-day groundwater flow system (McCartney, 1984; Thomas et al., 1998)	Reactivity of primary minerals:3 Fracture complexity: 1 Extent of wallrock alteration: 1 Groundwater fluxes: 1
Toki Granite	Mizunami, Gifu prefecture, central Japan	MIU-3/8	70	555	Medium-grained granite	Single major fracture, bordered by narrow fracture zone, c. 5 mm thick. Fracture surface coated by latest low temperature calcite-smectite (±pyrite). Wallrock more altered than the Carnmenellis Granite and BVG samples, but less than MIU-3/10	Reactivity of primary minerals:3 Fracture complexity: 2 Extent of wallrock alteration: 2 Groundwater fluxes: 3
Toki Granite	Mizunami, Gifu prefecture, central Japan	MIU-3/10	70	522	Medium-grained granite	More complex, broader fracture zone than MIU-3/8, c. 20 mm thick shows much alteration. Fracture surface mineralized by latest low temperature calcite-smectite (±pyrite) mineralization.	Reactivity of primary minerals:3 Fracture complexity: 3 Extent of wallrock alteration: 3 Groundwater fluxes: 3
Borrowdale Volcanic Group (BVG)	Near Sellafield, northwest England	SSK70953	455	1000	Dense meta-tuff	Steeply inclined fracture containing a complex calcite-dolomite-hematite vein of probable Permo-Triassic to Jurassic age (termed "ME6; Milodowski et al., 1998) with late Quaternary calcite overgrowths (termed "ME9"; Milodowski et al., 1998, 2018). Associated with fracture zone c. 30 mm across.	Reactivity of primary minerals:1 Fracture complexity: 1 Extent of wallrock alteration: 1 Groundwater fluxes: 2.
Borrowdale Volcanic Group (BVG)	Near Sellafield, northwest England	SSK70955	455	465	Dense meta-tuff	Planar hairline open fracture, with very thin calcite layer of Quaternary age ("ME9"; Milodowski et al., 1998) on reactivated surfaces of Permo-Triassic to Jurassic age calcite-hematite mineralization ("ME6"; Milodowski et al., 1998, 2018). Fine anastomosing hairline calcite- mineralized microfractures extend in wallrock for c. 5 mm	Reactivity of primary minerals:1 Fracture complexity: 2 Extent of wallrock alteration: 1 Groundwater fluxes: 2

models for radionuclide retardation might be generally applicable. A much larger sample set would be needed to prove the reverse, namely that a single model for radionuclide retardation processes exists or can be developed for application to all kinds of FCR. However, this was not the goal of the study.

3.2. Samples

Commensurate with meeting the objectives of the study the samples were required to: (i) cover a range of different higher strength rock types, both relatively coarse grained and relatively fine grained; (ii) include fractures with different characteristics, in terms of complexity and in terms of the associated mineral infills and wallrock alteration; (iii) coexist with groundwater having pressure-temperature-chemical characteristics similar to those likely to occur in the host rocks of a radioactive waste repository; and (iv) contain fractures that are likely to be hydraulically active within the present day groundwater flow regime.

All samples came from sites where the geology, geochemistry and hydrogeology have been investigated extensively. Each sample contains fractures, here termed "potentially flowing features" or "PFFs" to reflect their identification on petrographical/structural grounds as likely pathways for presently flowing groundwater (Milodowski et al., 1995, Milodowski et al., 1997). The complexity of the fracturing differs among the samples and the margins of the PFFs display varied degrees and types of alteration. Sample characteristics are summarized in Table 1.

3.2.1. Carnmenellis granite

The Carnmenellis Granite sample SSK70951 is of Carboniferous age and comes from borehole RH15, in Rosemanowes Quarry, Cornwall, UK, drilled during the 1980's for a geothermal project (Batchelor, 1987). The deviated borehole is drilled directly into granite at 164 m above sea level with a drilled length of 2810 m. Natural groundwater is recent meteoric water mixed with deeper, palaeo-meteoric water that has acquired high salinity (Total Dissolved Solids, TDS, to several thousand mg/L) due to water-rock reactions (Edmunds et al., 1984; Edmunds and Savage, 1991). The residence time of groundwater in the granite at the sampling location is unknown, but elsewhere the saline component of deep groundwater has resided in the granite in the order of 10^6 years (Edmunds et al., 1984). Traces of calcite-laumontite coating the fracture in sample SSK70951 represents low temperature mineralization (Jove and Hacker, 1997), possibly formed under the present-day active deep groundwater conditions (McCartney, 1984; Thomas et al., 1998).

3.2.2. Toki granite

The Toki Granite samples MIU-3/8 and MIU-3/10 come from borehole MIU-3, drilled by the Japan Nuclear Cycle Development Institute (JNC) at Shobasama, Mizunami, central Japan. The Cretaceous Toki Granite intrudes Jurassic sedimentary rocks of the Mino terrane (Wakita, 2000).

The borehole has a top at 230 m above sea level and is approximately vertical with a drilled length of 1014 m, the upper 88 m of which intersect Miocene marine and lacustrine sedimentary rocks of the Mizunami Group. The remainder is in the Toki Granite (Toyokura et al., 2000).

Groundwater in the borehole is meteoric in origin and was recharged up to 6 km to the northeast (JNC, 2004). Under a topographic head gradient groundwater flows through the granite past the MIU-3 borehole to discharge near the Toki River, about 2 km to the south. All groundwater at the Shobasama site is Na–HCO_3-dominated, with TDS up to c. 200 mg/L (Hasegawa et al., 2016). ^{14}C data suggest that groundwater has resided in the middle of the sedimentary sequence near the borehole for c. 9.3 ka, but for >50 ka in the deepest granite (c. 1000 m below ground level)(Iwatsuki et al., 2005). Groundwater samples from the MIU-3 borehole all contain ^{14}C, suggesting a component of the groundwater was recharged within the last c. 50 ka (Hasegawa et al., 2016).

The latest-mineralisation on the fracture surfaces of samples MIU-3/8 and MIU-3/10 is calcite (±smectite, pyrite) and correlates closely with present groundwater flow.

3.2.3. Borrowdale volcanic group (BVG)

The BVG samples SSK70953 and SSK70955 are fine-grained low-grade meta-tuffs of Ordovician depositional age. The samples were taken from boreholes RCM3 and BH9A respectively, near Sellafield in northwest England. These boreholes were drilled by Nirex during investigations in the 1990's for a (then) proposed geological repository for intermediate-level and some low-level radioactive waste (L/ILW) (Nirex, 1998a,b; Bath et al., 2006). Both boreholes are vertical, RCM3 being drilled from a point 102 m above sea level for 1035 m, and BH9A from a point 116 m above sea level for 500 m.

At borehole RCM3, Permo-Triassic sedimentary rocks c. 300 m thick cover the BVG but thicken westwards towards the East Irish Sea Basin (EISB) and reach 1600 m thick at the coast, about 3 km west-south-west of RCM3. Borehole BH9A is 2.5 km east-north-east of RCM3, where only thin superficial Quaternary glacial deposits cover the BVG (Nirex, 1998b; Bath et al., 2006).

Groundwater near the sampled rocks is Na–Ca–Cl dominated and saline, with TDS of c. 27,000 mg/L near SSK70953, and c. 20,000 mg/L near SSK70955 (Nirex, 1998b; Bath et al., 2006). Isotopic evidence suggests that this groundwater is predominantly of Pleistocene meteoric origin with a subsidiary component of saline water that has resided within the BVG for >1.5 Ma (Nirex, 1998b; Bath et al., 2006; Metcalfe et al., 2007). A topographic head gradient drives groundwater flow coastwards from uplands eastwards of BH9A (Bath et al., 2006; Nirex, 1998a,b; Metcalfe et al., 2007).

The earliest fracture mineralization in samples SSK70953 and SSK70955 is predominantly ferromanganoan calcite and subordinate dolomite-ankerite and hematite, associated with hematitisation (iron oxyhydroxide formation) in the adjacent wallrock. This mineralisation (the "ME6" mineralisation episode; Milodowski et al., 1998) formed from warm (53–180 °C) basinal Na–Ca–Cl–SO_4 hypersaline brines (~25 wt% salt equivalent) expelled from the EISB from the Permian to early Jurassic (Milodowski et al., 1998). The most recent mineralization episode ("ME9"; Milodowski et al., 1998, 2018) followed fracture reactivation and dilation. Ferromanganoan calcite occurs in presently open fractures, and isotopes of carbon, oxygen and strontium, fluid inclusion data and uranium-series dating, all indicate that it formed in the modern groundwater system.

4. Analytical methods

Core samples were firstly X-rayed to produce X-ray radiographs that identified fractures within the cores invisible to the naked eye. The images obtained were used to aid selection of sub-samples for more detailed analysis.

Thin sections were examined under plane-polarised light (PPL) and cross-polarised light (XPL), using a Zeiss AxioImager A2m polarizing microscope with a bespoke Zeiss AxioCam ICC5 digital camera.

Digital Autoradiography, Phosphor Imaging Plate (DAIP) autoradiographs were recorded by placing Fuji General Purpose polyurethane-coated Eu-doped barium fluorobromide (BaFBr) phosphor imaging plates (IP) on the cut core surfaces. The IPs were exposed to bright white fluorescent light for 20 min to erase energy from background radiation and then exposed to the samples for c. 29 days in a light-tight box. After removal in a darkroom, the IP was scanned with red laser light (635 nm) at 50 μm resolution to release sample radiation-induced energy in the phosphor, as photostimulated luminescence (PSL; Zeissler, 1997; Gonzalez et al., 2002). This process used an Amersham Biosciences (GE Healthcare Ltd) STORM 860 digital fluorescence scanner.

Etch Track Autoradiography (ETA) involved placing a piece of allyl diglycol carbonate monomer (ADC) plastic on the cleaned surface of a rock thin section (Basham et al., 1982). The ADC remained in contact with the rock surface for about 8 weeks and was then etched for 2–3 h using 6N NaOH, revealing individual tracks where the structure of the ADC had been damaged by single α-particles.

Samples for Inductively Coupled Plasma-Mass Spectrometry (ICP-MS) analyses were each prepared by digesting c. 100 mg of powdered rock in a mixture of ultrapure nitric acid and hydrofluoric acid. The resulting solutions were evaporated to dryness and then re-dissolved in 2% nitric acid before being re-evaporated to ensure hydrofluoric acid removal. All samples were re-dissolved in 50 mL of 2% nitric acid. Some contained precipitates, which were dissolved by adding 2 mL of concentrated hydrochloric acid. The samples were then analysed using an Agilent Technologies model 7500x ICP-MS fitted with a quartz double-pass spray chamber (Peltier-cooled, Scott-type), a concentric MicroMist nebuliser and a 3rd generation Octopole Reaction System (ORS3). The ICP-MS was optimised daily using a solution of Li, Mg, Y, Ce, Tl and Co (1 μg/L) in 2% (w/v) HNO_3 acid. Matrix interferences and signal drift within each run were corrected using analyses of a 100 mg/L internal standard solution of ^{45}Sc, ^{72}Ge, ^{103}Rh, ^{125}Te and ^{193}Ir. Standards were made from stock single and mixed element standards supplied by VWR and Johnson Matthey.

Energy Dispersive X-ray Analysis (EDXA) used a FEI QUANTA 600 environmental scanning electron microscope (ESEM) fitted with an Oxford Instruments INCA Energy 450 energy dispersive X-ray microanalysis (EDXA) system. This instrument had an Oxford Instruments X-MAX 50 mm^2 Peltier-cooled (liquid nitrogen free) silicon drift detector (SSD). Back-Scattered Electron Microscopy (BSEM) was used to make detailed high-resolution back-scattered electron images of the polished thin sections using the same instrumentation. These images allowed more petrographical relationships to be discerned.

5. Results and discussion

5.1. Carnmenellis granite

DAIP records abundant point-sources of relatively high radioactivity disseminated throughout the matrix of the Carnmenellis Granite (Fig. 2b). These sources correspond mostly to α- or β-particle emitters (i.e. U- or Th-rich minerals) exposed at the sample surface. Grains below the surface are undetected because α-, and to a lesser extent β-, particles are too rapidly attenuated by the rock, meaning that they have a very short range. In contrast, γ-rays from ^{40}K are much less attenuated and the autoradiographs therefore record γ-radiation from deeper in the sample as more diffuse areas of relatively high radioactivity.

The more radioactive point sources mostly coincide with clusters of biotite crystals (c.f. Fig. 2a and b). The most intense sources are probably inclusions of low-Th uraninite, which is a primary accessory mineral in the Carnmenellis Granite (Basham et al., 1982; Jefferies, 1984, 1985). Monazite, zircon, xenotime and apatite are also accessory minerals (Basham et al., 1982; Jefferies, 1984, 1985). All contain U and/or Th and are often associated with biotite, which may explain the less intense point sources in Fig. 2b.

A prominent radioactive band across the Carnmenellis Granite core (Fig. 2b) may be an early annealed microfracture with U mineralization. High-temperature hydrothermal uraninite mineralization occurs elsewhere in the Carnmenellis Granite (Jefferies, 1984).

More diffuse less radioactive patches occur throughout (Fig. 2b, light-blue areas), corresponding to K-feldspar and mica crystals exposed at the surface (Fig. 2a). Non-radioactive areas (darker blue) correspond to quartz and plagioclase. Allowing for the sample geometry, radioactivity in the rock matrix appears to be unrelated to the PFF (top of Fig. 2a).

Despite the secondary minerals on the fracture plane, the Carnmenellis Granite sample yields no evidence for redistribution of natural U, Th and K nor visible mineralogical alteration around the fracture.

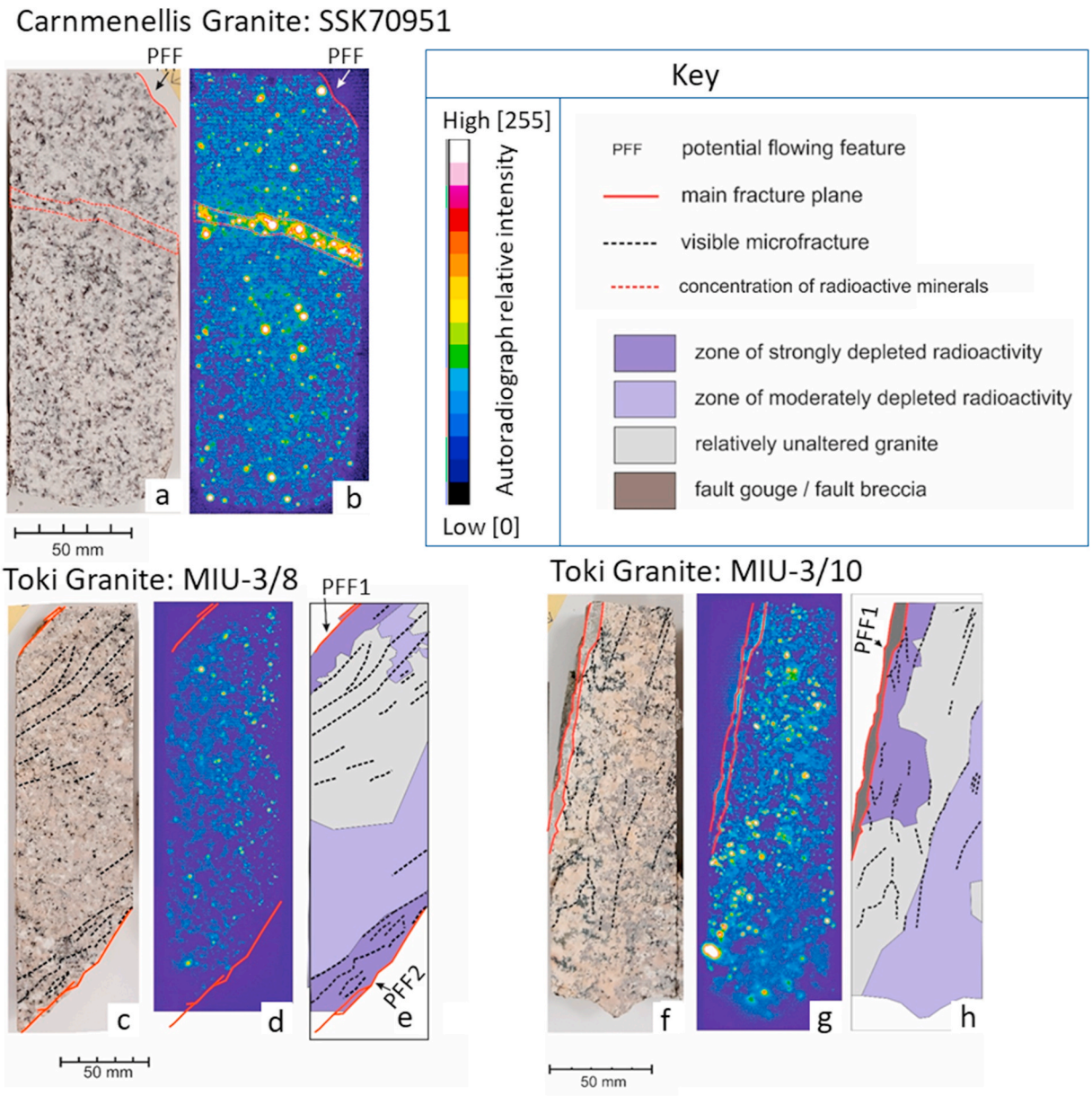

Fig. 2. Textures and structures (core photographs a, c and f), and cumulative total α-, β- and γ-radioactivity (DAIP b, d and g), in granite cores. Black crystals in a), c) and f) are biotite. In b), d) and g) relatively highly radioactive spots (red to white) are probably U- and Th- rich minerals, and more diffuse lower-intensity radioactivity (blue) is mostly γ-from K in K-feldspar, muscovite and biotite. A narrow radioactive band in the Carnmenellis Granite is unrelated to any obvious structure or texture (a, b). The Toki Granite samples have relatively low total radioactivity near the PFFs (d, e, g, h). Cores were half-cylinder slices, causing radioactivity to apparently decrease towards the autoradiograph margins.

5.2. *Toki granite*

The Toki Granite samples exhibit major alteration and mineralization related to the PFFs and associated microfractures, which extend up to 50 mm from the main fracture (Fig. 2). In both samples, fractures are filled or lined by calcite and calcic plagioclase cores have been extensively dissolved and replaced by calcite (±smectite).

Sample MIU-3/8 is weakly sheared, microfractures being developed parallel to the main fractures (Fig. 2c and e). DAIP (Fig. 2d) shows abundant, small, relatively radioactive sources, principally associated with primary igneous U- or Th-rich accessory minerals, and commonly occurring as inclusions in mafic mineral clusters. BSEM-EDXA identified these point sources as zircon and apatite which, together with ilmenite, magnetite, uranothorianite, and secondary allanite, are the principal accessory minerals in the main Toki Granite facies (Yuguchi et al., 2011, 2016; Nishimoto et al., 2014). Their chemistries indicate these radioactive sources to be α- and β-emitters.

Diffuse patches of lower radioactivity in sample MIU-3/8 (Fig. 2d) correspond to K-feldspar and mica, while quartz and plagioclase are non-radioactive. From its spatial correlation with K- minerals, the more diffuse radioactivity is apparently predominantly γ-, emitted by ^{40}K. The intensity of radioactivity decreases near the PFF (Figs. 2d and e). Spatial distributions of the point-sources and the more diffuse γ - sources correlate with alteration intensity and they are markedly scarcer next to the PFFs. We conclude that U (±Th) and K were leached from the altered wallrock adjacent to the fractures. The alteration coincides with microfracturing in the wallrock. This is particularly evident where the reduction in radioactivity corresponds to microfractured wallrock adjacent to PFF2 (Fig. 2d and e).

MIU-3/10 is mineralogically like MIU-3/8, but coarser grained and

more intensely altered, with alteration throughout the core. The wallrock matrix is strongly sheared with numerous microfractures parallel to the main fracture (Fig. 2f, g and h). Adjacent to the PFF, the wallrock is colored orange by finely disseminated secondary iron oxides. K-feldspar grains are coarsened by rims of white albite for up to 25 mm from the PFF (Fig. 2f).

The DAIP (Fig. 2g) is like that of sample MIU-3/8, relatively radioactive spots probably corresponding to uraniferous (and/or thoriferous) accessory minerals such as zircon, apatite and possibly allanite, in chloritized biotite aggregates. More diffuse, low-level radioactivity corresponds to K-feldspar. Quartz and plagioclase are not radioactive but may contain radioactive inclusions of accessory minerals (e.g. zircon, apatite, uranothorianite). Fault gouge adhering to the PFF surface is also less radioactive, with diffuse radioactivity (probably γ) associated with fragments of K-feldspar and clay matrix material (probably smectite). No radioactivity was detected in the calcite coating the fracture surface.

As in MIU-3/8, the radioactivity correlates with wallrock alteration. Near the PFF relatively highly radioactive point-sources are much less abundant, and diffuse low-level radioactivity associated with K-feldspar is lower. Radioactivity is lower for 5–35 mm from the main fracture, throughout a zone of microfracturing and partial K-feldspar argillisation (Fig. 2f, g, and h).

The autoradiograph of the altered wallrock shows diffuse, low-level radioactivity localized within fine microfractures. Some microfractures contain a very fine grained secondary REE phase (probably a carbonate), a potential U and Th host. The more radioactive spots occur principally within mafic aggregates of chloritized biotite (lower left of Fig. 2g).

ETA also shows a similar relationship in these samples, with fewer α-emitting sources fewer near the PFF than further away (Fig. 3).

5.3. Borrowdale volcanic group

Unlike the granite samples, the two BVG samples are very fine grained with radioactivity evenly distributed through the rock matrix (Fig. 4). The DAIP of SSK70953 shows a weak, diffuse distribution of total radioactivity (Fig. 4b). Most of the radioactivity is γ-activity, from K in muscovite and K-feldspar. No radioactivity was detected in calcite infills of either the PFFs or microfractures cutting the matrix (Fig. 4b and c).

Chlorite patches adjacent to PFF1 and PFF2 show slightly higher radioactivity (Fig. 4b and c). This radioactivity is diffusely distributed within the chlorite, but also occurs in very fine spots corresponding to secondary hematite alteration.

Chlorite hematitisation, which weakly reddens the fracture wallrock, and associated diffuse enhancement of radioactivity, coincide with microfractures that extend for 10–50 mm from the main fracture surfaces. This well-defined zone of localized intense microfracturing was imaged by X-ray radiography but is not readily visible in the hand specimen.

The other BVG sample, SSK70955, shows γ-radioactivity variations parallel to the rock's cleavage, probably from K in muscovite (white

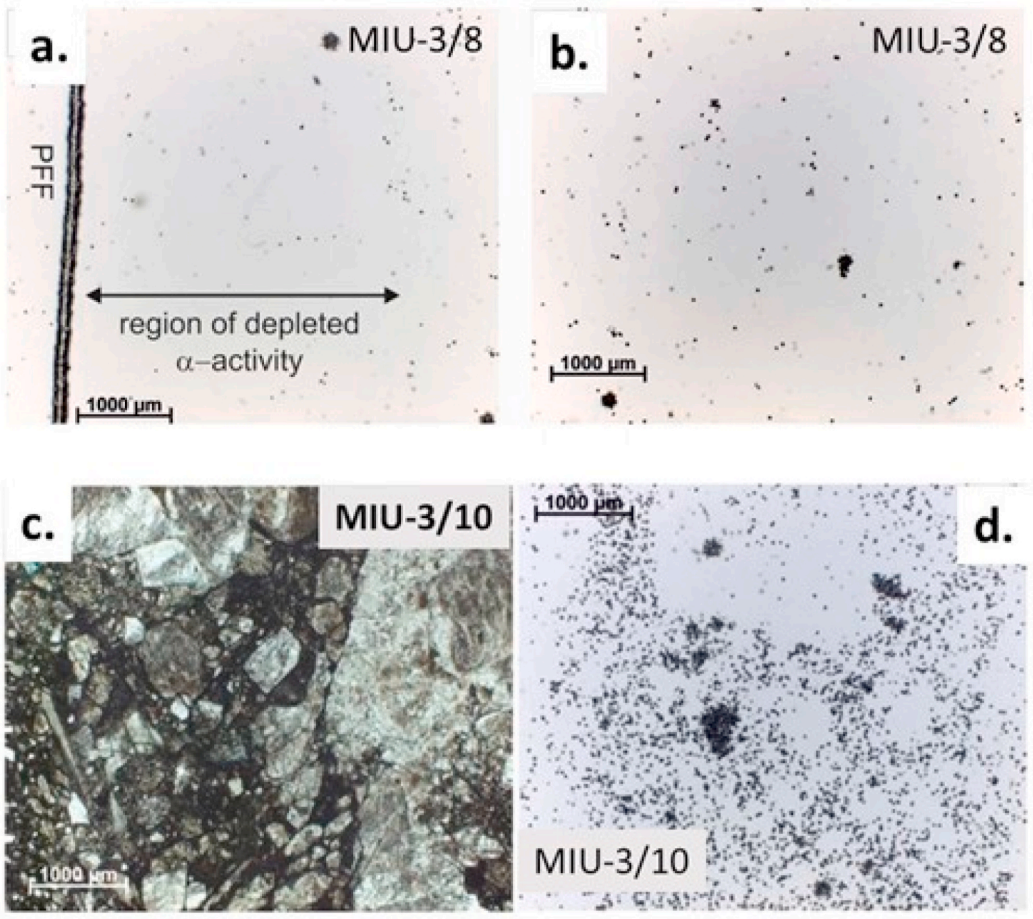

Fig. 3. Radioactivity distribution in Toki granite samples relative to alteration. a. ETA of an area of sample MIU-3/8 illustrating a narrow zone of relatively low α-radioactivity immediately adjacent to the PFF, which contrasts with b.. ETA showing background α-radioactivity 4–8 mm distant from the PFF in Toki Granite sample MIU-3/8. c. Optical photomicrograph (PPL) of part of the shear zone in the wallrock of the PFF in Toki Granite sample MIU-3/10, showing finely comminuted host rock particles in a dark clay-rich matrix. d. ETA of the same area showing more prominent and diffuse α-tracks within the fine matrix. Occasional discrete radioactive spots correspond to coarse fragments of primary igneous bastnaesite entrained within the gouge.

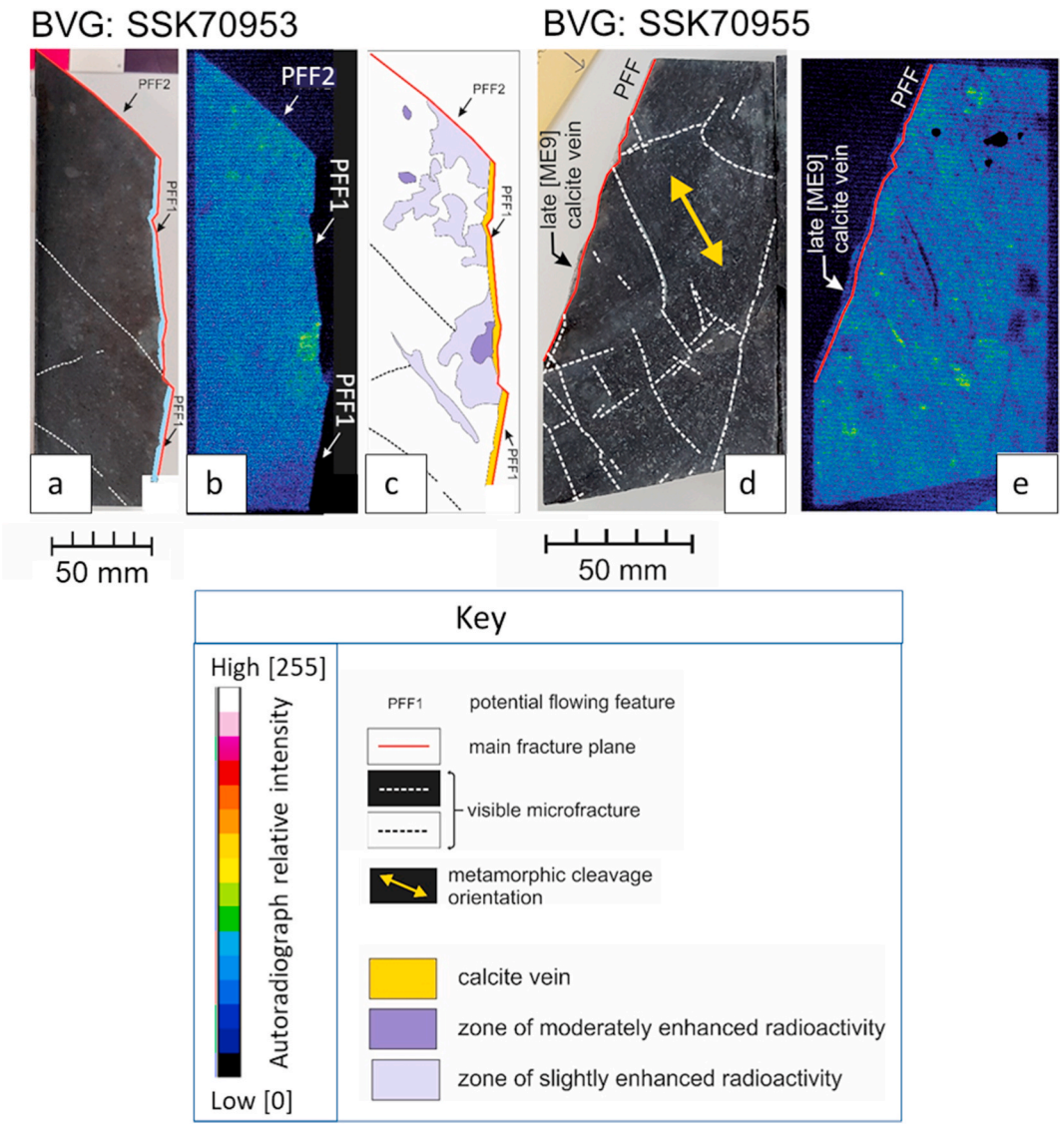

Fig. 4. Textures and structures (core photographs a,c and d), and distributions of cumulative total α-, β- and γ-radioactivity (DAIP, b and e), in BVG samples SSK70953 (a,b,c) and SSK70955 (d, e). In the autoradiographs, brighter areas are more radioactive than darker areas. In SSK70953 locally enhanced but diffuse radioactivity (green to yellow) is associated with weakly hematitised patches of chlorite in the rock matrix. (b, c). In SSK70955 the autoradiograph shows radioactivity to be distributed parallel to the cleavage in addition to localised patches of weakly-hematitised chlorite (d, e), but there is no relationship between the radioactivity and the PFF. (For interpretation of the references to color in this figure legend, the reader is referred to the Web version of this article.)

mica) and K-feldspar (Fig. 4d and e). Segregation of muscovite into domains in the cleavage causes the alignment. The calcite-mineralized microfractures are distinguished in the autoradiograph by their lack of radioactivity. No obvious changes in wallrock radioactivity occur adjacent to the PFF, implying negligible migration of radioactive elements (U, Th and K) into, or out of, the wallrock.

5.4. Comparison of samples

Across the Toki Granite, BVG and Carnmenellis Granite samples, spatial variations in radioactivity near potentially flowing fractures (PFFs) correlate with mineralogical alteration of fracture wallrocks. Fracture walls in the Carnmenellis Granite sample and the two BVG samples show little alteration and in these samples the intensity of radiation and the frequencies of discrete radioactive sources do not vary significantly with distance from the fractures. In contrast, the two Toki Granite samples are much more intensely altered and in these both the overall intensity of radiation and the numbers of discrete radioactive sources are lower in more intensely altered and micro-fractured zones near to the main PFFs.

In both the Carnmenellis Granite sample and the two BVG samples, the distribution of α-radiation mirrors that of total radiation and is consistent with little variation in the concentrations of U and Th in bulk rock samples and fracture infills (Fig. 5). Fracture wallrocks show some redistribution of radioactive elements where there is mineralogical alteration, but vein fills contain little radioactivity.

In the two Toki Granite samples, the variations in radioactivity are consistent with lower concentrations of U and Th in altered rock and fracture infills compared to less altered rock (Fig. 5). These observations can be explained by the mineralogical alteration being accompanied by migration and loss of U (±Th) and K in the altered rock. This alteration extends for at least 50 mm from major fractures in the studied Toki Granite cores.

The less altered Toki Granite sample, MIU-3/8, has fewer α-emitters in the matrix near the PFF than occur further away (c.f. Fig. 3a and b), consistent with the DAIP image and the U and Th analyses (Fig. 5). In contrast, although Toki Granite sample MIU-3/10 similarly has low total radioactivity near the PFF (Fig. 2g and h), and is likewise depleted in U

and Th (Fig. 5), the α-radioactivity is relatively high in the altered wallrock by the PFF (c.f. Figs. 2g and 3d). We infer that the altered wallrocks of the PFFs in this very fractured sample have taken up another α-emitting nuclide, confirmed by γ-spectrometry to be ^{226}Ra. Given the relatively short half-life of ^{226}Ra (~1600 years) this uptake must have occurred in the recent geological past and could be continuing at present. Much of the secondary concentration of radioactivity is associated with extensive smectitic and chloritic alteration of the highly microfractured wallrock (Fig. 3c and d), and possibly the ^{226}Ra has been adsorbed here. The ^{226}Ra could also have been uptaken by the calcite that occurs extensively in the wallrock adjacent to the fracture in this sample. This latter possibility implies that formation of calcite is at least in part recent.

6. Conclusions

In the five studied samples little evidence exists for migration of radioactive elements between fractures and their wallrocks except where mineralogical alteration of primary minerals has occurred in association with extensive microfracturing. In the two most altered samples, from the Toki Granite, there is evidence for U and Th being lost from the rock during this alteration, but also, in the most intensely altered part of one sample, for ^{226}Ra uptake from groundwater within the last few thousand years. The extents of sample alteration can be related to both the porosity-permeability characteristics of the rock and to the groundwater flow regimes within the rocks. The minerals in the Carnmenellis Granite are reactive with groundwater at present conditions, but geologically ancient alteration at relatively high-temperatures has sealed the porosity, thereby limiting interactions between more recent, lower-temperature flowing waters and the rock. It can be inferred from the hydraulic setting and regional groundwater chemistry that present groundwater fluxes are the lowest of any of the sampled sites. The BVG samples are fine grained and have also undergone geologically ancient alteration. In combination these factors have produced poorly interconnected porosity, which has restricted access of the rock matrix to water flowing in fractures, even though groundwater actively flows through fractures. The Toki Granite, the youngest of the examined rocks, has relatively high fracture porosity and connectivity. Fresh groundwater flows relatively rapidly through the fractures, driven by a steep hydraulic gradient. These characteristics, and reactive minerals in the granite, have caused intense alteration.

Several features of our results are not predicted by existing RMD models such as the one shown in Fig. 1. Firstly, we found a marked association of radionuclide addition or removal with mineralogical alteration related to the PFFs in the Toki Granite samples. Secondly, only a single reaction front is observed in all the samples (the fronts in the BVG and Carnmenellis Granite being very close to the studied PFFs). If solutes were added or removed to a uniform matrix by diffusive exchange with fracture fluids, different solutes should be transported by different amounts according to their concentration and transport properties, causing a series of spaced "fronts". In the cases that we have identified, RMD appears to have been coupled to mineralogical alteration and microfracturing, which limits the spatial extent of the reaction front. This situation contrasts with the model in Fig. 1 in which the rock matrix has temporally invariant physical and chemical properties. In this earlier model water/rock reactions do not occur to the extent that the rock properties controlling radionuclide retardation evolve significantly.

The results from the Toki Granite suggest that alteration could occur sufficiently rapidly to significantly change the ability of a rock matrix to support RMD on safety assessment timescales (typically 10^5–10^6 years). These results are supported X-ray computed tomography and microfocus synchrotron X-ray Fluorescence mapping reported elsewhere (Wogelius et al., 2020). Some changes would tend to enhance RMD (porosity generation by mineral dissolution), while other changes would tend to reduce RMD (porosity occlusion by secondary mineral precipitation and/or formation of lower density phases). This possibility is not covered by any of the established models. Further work is required to determine whether on-going alteration could indeed be relevant to safety assessment and if so, under what circumstances.

Thirdly, the abundant fresh biotite in the Carnmenellis granite is inconsistent with fracture wall rocks always containing connected, water-saturated porosity. At the prevailing conditions, biotite is unstable in the presence of water, hydrating to chlorite + K-feldspar (Wilson, 2004; Brady et al., 2019). The lack of alteration of biotite in the deep granite implies that it was not always water saturated. If so, then much of the matrix porosity would be inaccessible to solutes and hence irrelevant for RMD. Presently, little observational or experimental data on this point exists and further evaluation is needed.

We have developed a model to reflect the observations of the present study (Fig. 6).

In this model an altered zone with enhanced porosity and permeability exists around the central fracture and transport is predominantly fracture-parallel. Beyond the zone, any transport is by orthogonal diffusion. The abrupt change in transport properties at the edge of this altered zone causes superimposed transport fronts for most mobile components, a pattern that is well known from a variety of natural geological settings (Balashov and Yardley, 1998; Skelton et al., 2000; Lewis et al., 1998). Both diffusion and advection are possible within the altered "damage zone". For example, enhanced porosity very near the fractures was noted in earlier studies of BVG samples (Baker et al., 2002), but it was not appreciated that juxtaposed "fronts" for a range of components are inconsistent with simple diffusion and reflect fracture-parallel advection. The only alteration in the fracture walls in BVG samples is hematitisation (occurrence of iron oxy-hydroxides). According to the model presented here, there was no transport beyond the reddening front that indicates its limit.

The altered damage zone around the main fracture is a key feature of the model and dictates the rock volume which allows radionuclide

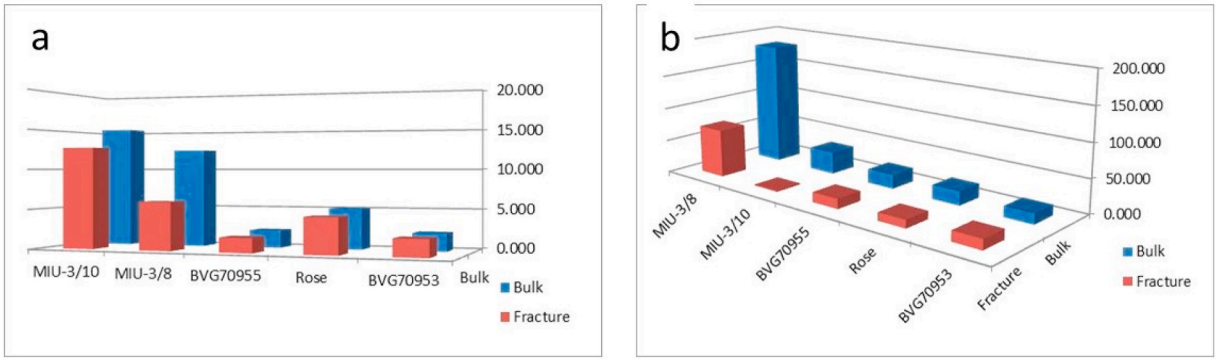

Fig. 5. Comparison of U (a) and Th (b) concentrations (ppm) in bulk samples and fracture-dominated sub-samples of the five specimens used in this study. b. All analyses by ICP-MS.

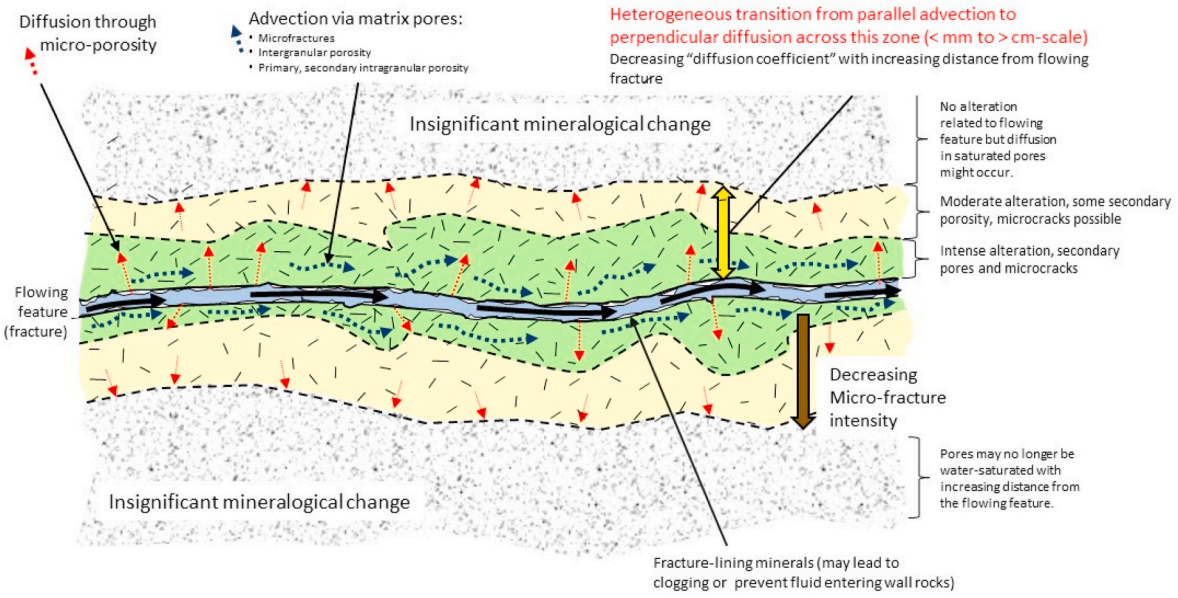

Fig. 6. Conceptual model for radionuclide uptake in the studied FCR samples, assuming that dissolved radionuclide concentrations are higher in the fracture than in the matrix porewater (the direction of radionuclide diffusion will reverse if concentrations of dissolved radionuclides transported through the fracture decrease to below the concentrations in the rock matrix pores). Even within the small sample suite investigated, the relative thickness of the different zones clearly varies significantly, and it is not always possible to distinguish more than one altered zone.

ingress by RMD. The spatial extent of alteration and its intensity depend on the frequency and connectivity of microfractures around the main fracture, and the porosity generated during mineralogical alteration. The latter depends on the chemistry and fluxes of inflowing groundwater, and the reactivity of the rock matrix. In the present study the altered damaged zones were greatest in the Toki Granite samples, extending for up to a few tens of millimetres of the main fractures.

The mineralogical alteration rates are not water supply-limited, and some water will continue to move through the altered zone without participating in reactions. Excess water returned to the fracture may still transport much of its dissolved load, although radionuclides may be adsorbed to existing grains or incorporated in new minerals, as for ^{226}Ra in sample MIU-3/10.

Water penetrating slowly into fresh rock will be consumed by hydration reactions. If, as a result, the pores are not filled by a continuous water film, diffusion through the rock will be much slower than measurements made on water-saturated rock, suggest.

While only a small sample suite was studied, the results show that RMD may differ in significance in different kinds of FCR. Site-specific information is therefore needed to determine how much reliance can be placed on RMD when developing a safety case.

Declaration of competing interest

The authors declare the following financial interests/personal relationships which may be considered as potential competing interests: Profs. Wogelius and AE Milodowski and Dr Field have received research funding from RWM Ltd. Prof. Yardley and Drs. Metcalfe and Carpenter have received research funding from, and provided technical consultancy under contract to, RWM Ltd. Prof. Yardley was formerly employed as Chief Geologist by RWM Ltd. Dr. Norris is employed by RWM Ltd. as a senior research manager.

Acknowledgements

A.E. Milodowski and L.P. Field publish with the permission of the Executive Director of the British Geological Survey (UKRI). JAEA is thanked for allowing the Toki Granite core samples to be investigated. Dr K. Hama is thanked for helpful discussions concerning these samples. Dr A.H. Bath is thanked for helpful editorial comments and two anonymous reviewers are thanked for helpful review comments. The work was funded by Radioactive Waste Management Limited.

References

Ahonen, L., Kaija, J., Paananen, M., Hakkarainen, V., Ruskeeniemi, T., 2004. Palmottu Natural Analogue: A Summary of the Studies. Geological Survey of Finland Report. YST-121.

Alexander, W.R., Frieg, B., Ota, K. (Eds.), 2009. Grimsel Test Site Investigation Phase IV the Nagra-JAEA in Situ Study of Safety Relevant Radionuclide Retardation in Fractured Crystalline Rock III: the RRP Project Final Report. Nagra Technical Report, NTB 00-07. Nagra, Baden, Switzerland.

Baker, A.J., Jackson, C.P., Jefferies, N.L., Lineham, T.R., 2002. The Role of Rock Matrix Diffusion in Retarding the Migration of Radionuclides from a Radioactive Waste Repository. United Kingdom Nirex Limited Report N/051. United Kingdom Nirex Limited, Harwell, Oxfordshire, UK.

Balashov, V.N., Yardley, B.W.D., 1998. Modeling metamorphic fluid flow with reaction-compaction-permeability feedbacks. Am. J. Sci. 298, 441–470.

Basham, I.R., Ball, T.K., Beddoe Stephens, B., Michie, McL.U., 1982. Uranium-bearing accessory minerals and granite fertility: II Studies of granites from the British Isles. In: Uranium Exploration Methods. International Atomic Energy Agency, Vienna, pp. 398–411.

Batchelor, A.S., 1987. Development of hot-dry-rock geothermal systems in the UK. IEEE Proc. 134, 371–380.

Bath, A.H., Richards, H.G., Metcalfe, R., McCartney, R.C., Degnan, P., Littleboy, A.H., 2006. Geochemical indicators of deep groundwater movements at Sellafield. UK. J. Geochem. Explor. 90, 24–44.

Bear, J., Tsang, C.-F., de Marsilly, G., 1993. Flow and Contaminant Transport in Fractured Rock. Academic Press Limited, London.

Brady, P., Lopez, C., Sassani, D., 2019. Granite hydrolysis to form deep brines. Energies 12, 2180. https://doi.org/10.3390/en12112180.

Edmunds, W.M., Andrews, J.N., Burgess, W.G., Kay, R.L.F., Lee, D.J., 1984. The evolution of saline and thermal groundwaters in the Carnmenellis Granite. Min. Mag. 48, 407–424.

Edmunds, W.M., Savage, D., 1991. Geochemical characteristics of groundwater in granites and related crystalline rocks. In: Downing, D.A., Wilkinson, W. (Eds.), B. Applied Groundwater Hydrology. Oxford University Press, pp. 266–282.

Gonzalez, A.L., Li, H., Mitch, M., Tolk, N., Duggan, D.M., 2002. Energy response of an imaging plate exposed to standard beta sources. Appl. Radiat. Isot. 57, 875–882.

Hasegawa, T., Nakata, K., Tomioka, Y., Goto, K., Kashiwaya, K., Hama, K., Iwatsuki, T., Kunimaru, T., Takeda, M., 2016. Cross-checking groundwater age by 4He and 14C dating in a granite, Tono area, central Japan. Geochem. Cosmochim. Acta 192, 166–185.

IAEA, 2001. The use of scientific and technical results from underground research laboratory investigations for the geological disposal of radioactive waste. In:

International Atomic Energy Agency Report IAEA-TECDOC-1243. International Atomic Energy Agency, Vienna.
Ikonen, J., Sardini, P., Siitari-Kauppi, M., Martin, A., 2017. In situ migration of tritiated water and iodine in Grimsel granodiorite, part II: assessment of the diffusion coefficients by TDD modelling. J. Radioanal. Nucl. Chem. 311, 339–348.
Iwatsuki, T., Furue, R., Mie, H., Ioka, S., Mizuno, T., 2005. Hydrochemical baseline condition of groundwater at the Mizunami underground research laboratory (MIU). Appl. Geochem. 20, 2283–2302.
Jefferies, N.L., 1984. The radioactive accessory mineral assemblage of the Carnmenellis granite. Cornwall. Procs. Ussher Soc. 6, 35–40.
Jefferies, N.L., 1985. Uraninite in the Carnmenellis pluton, Cornwall. In: High Heat Production (HHP) Granites, Hydrothermal Circulation and Ore Genesis. Proceedings of Conference Organised by the Inst Mining and Metallurgy, St Austell, Cornwall, England, 22-25 September 1985. Inst. Min. Metall. London, pp. 163–168.
JNC, 2004. Research Connected with the Development of Deep Geological Disposal for High Level Radioactive Waste: H15 (2004) Report, JNC Report TN1400 2004-007. Japan Nuclear Cycle Development Institute, Tokai Mura, Ibaraki, Japan.
Jove, C., Hacker, B.R., 1997. Experimental investigation of laumontite → wairakite + H2O: a model diagenetic reaction. Am. Mineral. 82, 781–789.
Kemppainen, M., Oila, E., Siitari-Kauppi, M., Sardini, P., Hellmuth, K.-H., 2001. Surveying for migration pathways in the granitic rock using nuclear track detectors, autoradiography and digital image analysis as an aid to construct the basis for heterogeneous diffusion modelling. In: Hart, K.P., Lumpkin, G.R. (Eds.), Scientific Basis for Nuclear Waste Management XXIV, Mater. Res. Soc. Symp. Proc, vol. 663, pp. 999–1006.
Lewis, S., Holness, M., Graham, C.M., 1998. Ion microprobe study of marble from Naxos, Greece: grain-scale fluid pathways and stable isotope equilibration during metamorphism. Geology 26, 935–938.
Marcos, N., Siitari-Kauppi, M., Suksi, J., Rasilainen, K., Finch, R., Hellmuth, K., 2000. Discussion on the use of matrix diffusion model after a multidisciplinary study of a granitic boulder sample. In: Hart, K.P., Lumpkin, G.R. (Eds.), Scientific Basis for Nuclear Waste Management XXIV, Mater. Res. Soc. Symp. Proc, vol. 663, pp. 1053–1063.
Markovaara-Koivisto, M., Marcos, N., Read, D., Lindberg, A., Siitari-Kauppi, M., Loukola-Ruskeeniemi, K., 2008. Release of U, REE and Th from Palmottu granite. In: William, E., Lee, W.E., Roberts, J.W., Hyatt, N.C., Grimes, R.W. (Eds.), Mater. Res. Soc. Symp. Proc. XXXI, vol. 1107, pp. 637–644.
McCartney, R.A., 1984. A geochemical investigation of two Hot-Dry Rock geothermal reservoirs in Cornwall, UK. PhD Thesis. Camborne School of Mines, Pool, Redruth, Cornwall, UK, p. 395pp.
Metcalfe, R., Crawford, M.B., Bath, A.H., Littleboy, A.K., Degnan, P.J., Richards, H.G., 2007. Characteristics of deep groundwater flow in a basin marginal setting at Sellafield, Northwest England: 36Cl and halide evidence. Appl. Geochem. 22, 128–151.
Miller, W.M., Alexander, W.R., Chapman, N.A., McKinley, I.G., Smellie, J.A.T., 2000. Geological disposal of radioactive wastes and natural analogues. In: Waste Management Series, vol. 2. Pergamon, Amsterdam, The Netherlands.
Milodowski, A.E., Gillespie, M.R., Naden, J., Fortey, N.J., Shepherd, T.J., Pearce, J.M., Metcalfe, R., 1998. The petrology and paragenesis of fracture mineralisation in the Sellafield area, west Cumbria. Proc. Yorks. Geol. Soc. 52, 215–241.
Milodowski, A.E., Gillespie, M.R., Shaw, R.P., Bailey, D.E., 1995. Flow-zone characterisation: mineralogical and fracture orientation characteristics in the PRZ and Fleming Hall Fault Zone area boreholes, Sellafield. In: Nirex Report, SA/95/001. United Kingdom Nirex Limited, Harwell, Oxfordshire, UK.
Milodowski, A.E., Barnes, R.P., Phillips, E.R., Shaw, R.P., 1997. Summary Data Compilation for the Location, Distribution and Orientation of Potential Flowing Features in the Sellafield Boreholes. Nirex Report, SA/97/031. United Kingdom Nirex Limited, Harwell, Oxfordshire, UK. United Kingdom Nirex Limited, Harwell, Oxfordshire, UK.
Milodowski, A.E., Bath, A.H., Norris, S., 2018. Palaeohydrogeology using geochemical, isotopic and mineralogical analyses: salinity and redox evolution in a deep groundwater system through Quaternary glacial cycles. Appl. Geochem. 40–60.
Mutch, R.D., Scott, J.I., Wilson, D.J., 1993. Cleanup of fractured rock aquifers: implications of matrix diffusion. Environ. Monit. Assess. 24, 45–70.
NEA, 2013. Underground research laboratories (URL). Nuclear Energy Agency, Organisation for Economic Cooperation and Development Report No. 78122. NEA/OECD, Paris, France.
Neretnieks, I., 2017. Solute Transport in Channel Networks with Radial Diffusion from Channels in a Porous Rock Matrix, SKB Report R-15-02. Swedish Nuclear Fuel and Waste Management Company, Stockholm, Sweden.
Nirex, 1998a. Sellafield Geological and Hydrogeological Investigations: the Hydrogeology of the Sellafield Area, 1997 Update. United Kingdom Nirex Science Report S/97/008. United Kingdom Nirex Limited, Harwell, Oxfordshire, UK.
Nirex, 1998b. Sellafield Geological and Hydrogeological Investigations: the Hydrochemistry of Sellafield, 1997 Update. United Kingdom Nirex Science Report S/97/089. United Kingdom Nirex Limited, Harwell, Oxfordshire, UK.
Nishimoto, S., Yoshida, H., Asahara, Y., Tsuruta, T., Ishibashi, M., Katsuta, N., 2014. Episyenite formation in the Toki granite, central Japan. Contrib. Mineral. Petrol. 167, 960–972.
Posiva, 2013. Safety Case for the Disposal of Spent Nuclear Fuel at Olkiluoto – Performance Assessment, 2012. Posiva Report Posiva 2012-04. Posiva Oy, Olkiluoto, Finland.
Poteri, A., 2009. Summary Report on the Up-Scaling of the Retention Properties by Matrix Diffusion in Fractured Rock, Posiva Working Report 2009-01. Posiva Oy, Olkiluoto, Finland.
Poteri, A., Nordman, H., Pulkkanen, V.-M., Smith, P., 2014. Radionuclide Transport in the Repository Near-Field and Far-Field. Posiva Report 2014-02. Posiva Oy, Olkiluoto, Finland.
Poteri, A., Andersson, P., Nilsson, K., Byegård, J., Skålberg, M., Siitari-Kauppi, M., Helarriuta, K., Voutilainen, M., Kekäläinen, P., Ikonen, J., Sammaljärvi, J., Lindberg, A., Timonen, J., Kuva, J., Koskinen, L., 2018. The First Matrix Diffusion Experiment in the Water Phase of the REPRO Project: WPDE 1. Posiva Working Report 2017-23. Posiva Oy, Olkiluoto, Finland.
Read, D., Black, S., Buckby, T., Hellmuth, K.-H., Marcos, N., Siitari-Kauppi, M., 2008. Secondary Uranium mineralization in southern Finland and its relationship to recent glacial events. Global Planet. Change 60, 235–249.
RWM, 2016. Geological disposal generic environmental safety case - main report. In: Nuclear Decommissioning Authority Report No. DSSC/203/01. Radioactive Waste Management Limited, Harwell, Oxfordshire, UK.
Sharp, J.M. (Ed.), 2014. Fractured Rock Hydrogeology. CRC Press, Boca Raton.
SKB, 2010. Radionuclide Transport Report for the Safety Assessment SR-Site. SKB Technical Report TR-10-50. Swedish Nuclear Fuel and Waste Management Company, Stockholm, Sweden.
Skelton, A.D.L., Valley, J.W., Graham, C.M., Bickle, M.J., Fallick, A.E., 2000. The correlation of reaction and isotope fronts and the mechanism of metamorphic fluid flow. Contrib. Mineral. Petrol. 138, 364–375.
Tachi, Y., Ebina, T., Takeda, C., Saito, T., Takahashi, H., Ohuchi, Y., Martin, A.J., 2015. Matrix diffusion and sorption of Cs+, Na+, I- and HTO in granodiorite: laboratory-scale results and their extrapolation to the in situ condition. J. Contam. Hydrol. 179, 10–24.
Thomas, L.J., Bromley, A.V., Milodowski, A.E., Kay, R.L.F., 1998. Alteration mineralogy. In: Edmunds, W.M., Andrews, J.N., Bromley, A.V., Kay, R.L.F., Milodowski, A.E., Savage, D., Thomas, L.J. (Eds.), Granite - Water Interactions in Relation to Hot Dry Rock Geothermal Development. Investigation of the Geothermal Potential of the UK. British Geological Survey, Keyworth, Nottingham, UK, pp. 57–80.
Toyokura, I., Hashii, T., Nagoe, S., Ito, T., Sugimori, T., Sugita, N., Masaeda, H., 2000. Hydrogeological Investigations in the Shobasama Site – MIU-3 Borehole. JNC Report JNC TJ7440 000-022. Japan Nuclear Cycle Development Institute, Tokai Mura, Ibaraki, Japan (In Japanese).
Vilks, P., Cramer, J.J., Jensen, M., Miller, N.H., Miller, H.G., Stanchell, F.W., 2003. In situ diffusion experiment in granite: phase I. J. Contam. Hydrol. 61, 191–202.
Voutilainen, M., Miettinen, A., Sardini, P., Parkkonen, J., Sammaljärvi, J., Gylling, B., Selroos, J.-O., Yli-Kaila, M., Koskinen, L., Siitari-Kauppi, M., 2019. Characterization of spatial porosity and mineral distribution of crystalline rock using X-ray micro computed tomography, C-14-PMMA autoradiography and scanning electron microscopy. Appl. Geochem. 101, 50–61.
Wakita, K., 2000. Melanges of the Mino terrane. Geol. Soc. Jpn. Mem. 55, 145–163 (in Japanese with English abstract).
Wilson, M.J., 2004. Weathering of the primary rock-forming minerals: processes, products and rates. Clay Miner. 39, 233–266.
Winberg, A., Andersson, P., Byegård, J., Poteri, A., Cvetkovic, V., Dershowitz, W., Doe, T., Hermanson, J., Gómez-Hernández, J.J., Hautojärvi, A., Billaux, D., Tullborg, A.-L., Holton, D., Meier, P., Medina, A., 2003. Final Report of the TRUE Block Scale Project 4. Synthesis of Flow, Transport and Retention in the Block Scale. Swedish Nuclear Fuel and Waste Management Company, Stockholm, Sweden. SKB Report TR-02-16.
Wogelius, R.A., Milodowski, A.E., Field, L.P., Metcalfe, R., Lowe, T., van Veelen, A., Carpenter, G., Norris, S., Yardley, B., 2020. Mineral reaction kinetics constrain the length scale of rock matrix diffusion. Nat. Sci. Rep. 10, 8142.
Yuguchi, T., Iwano, H., Kato, T., Sakata, S., Hattori, K., Hirata, T., Sueoka, S., Danhara, T., Ishibashi, M., Sasao, E., Nishiyama, T., 2016. Zircon growth in a granitic pluton with specific mechanisms, crystallisation temperatures and U-Pb ages: implications of "spatiotemporal" formation process of the Toki Granite, central Japan. J. Mineral. Petrol. Sci. 111, 9–34.
Yuguchi, T., Tsuruta, T., Nishiyama, T., 2011. Three-dimensional cooling pattern of a granitic pluton I: the study of exsolution sub-solidus reactions in the Toki granite, Central Japan. J. Mineral. Petrol. Sci. 106, 61–78.
Zeissler, C.J., 1997. Comparison of semiconductor pixel array, phosphor plate, and track etch detectors for alpha autoradiography. Nucl. Instrum. Methods Phys. Res. A392, 249–253.